



The chemical evolution of the Milky Way: a problem of Galactic archaeology

Galactic archaeology

F. Matteucci^{1,2,3,4}

¹ Università degli Studi di Trieste, Dipartimento di Fisica, Via Valerio 2, 34127, Trieste, Italy

² I.N.A.F., Osservatorio Astronomico di Trieste, via G.B. Tiepolo, 11, 34131, Trieste, Italy

³ I.N.F.N., Sezione di Trieste, Via Valerio, 2, 34127 Trieste, Italy

⁴ IFPU, Institute for the Fundamental Physics of the Universe, Via Beirut, 2, 34151, Trieste, Italy e-mail: francesca.matteucci@inaf.it

Received: 21-11-2022; Accepted: 23-01-2023

Abstract. We present and discuss some highlights in the chemical evolution of the Milky Way. Data from recent spectroscopic surveys are presented together with predictions of chemical evolution models aimed at explaining the observed abundance patterns. The basic ingredients to build chemical models for the Milky Way are discussed, namely the star formation history (star formation rate and initial mass function), the stellar yields and possible inflows and outflows. Concerning the stellar yields, we discuss the chemical enrichment from low, intermediate and massive stars, as well as merging white dwarfs (supernovae Ia) and merging neutron stars (kilonovae). Results concerning α -element evolution in the thick and thin disk stars are presented, together with results for the Galactic bulge. The evolution of Li abundance in the Milky Way is also discussed. From the comparison theory-observations we then derive constraints on stellar nucleosynthesis and formation of the various Galactic components.

Key words. Stars: Abundances, The Galaxy: evolution

1. Introduction

During the Big Bang only light elements formed (H, D, ^3He , ^4He , ^7Li), while the heavier elements from ^{12}C up to uranium and beyond were formed inside stars. The remaining light elements (^6Li , Be, B) have been formed by spallation (interaction of cosmic rays with C,N,O atoms in the interstellar medium). Elements from C to Fe were formed

by means of fusion reactions, whereas the elements heavier than Fe formed by neutron capture on Fe and other heavy seeds. This capture can be slow or rapid, relative to the timescale of the β -decay inside nuclei, thus giving rise to *s-process* and *r-process* elements.

Galactic archaeology studies the chemical abundances in Galactic stars and try to interpret them in terms of Galaxy for-

mation and evolution. The observed abundances and abundance ratios of the most common chemical elements represent a powerful tool to constrain either the stellar yields or the timescales of formation of the various Galactic components (halo, thick-, thin-disk and bulge). Precise stellar spectroscopy is necessary to Galactic archaeology and recently Large Galactic Surveys (e.g. APOGEE, Gaia-ESO, GALAH, AMBRE) have provided a great deal of stellar spectroscopic data. At the same time many Galactic chemical evolution models were aimed at reproducing the observed abundance patterns (see Matteucci (2021a), for a recent review). Here we will describe some of the results obtained by such models compared to observations.

Chemical evolution models contain some basic ingredients: i) the star formation history, which is the convolution of the star formation rate (SFR) and the initial mass function (IMF); ii) the stellar yields, namely the amounts of mass produced and ejected by stars in the form of chemical elements. Massive stars ($M > 10M_{\odot}$) are responsible for the production of the bulk of α -elements (C, O, Ne, Mg, Si, Ca) and part of Fe, which are ejected via a core-collapse (C-C) explosion (SNe II, Ib, Ic), while low and intermediate mass stars ($0.8 \leq M/M_{\odot} \leq 8.0$) are responsible for the formation of N and heavy s-process elements and eject their material during the planetary nebula (PN) formation. The bulk of iron is instead produced by SNeIa, namely exploding white dwarfs in binary systems. Concerning r-process elements either CC-SNe or merging neutron stars (MNS) can be responsible of their production (see Matteucci et al. (2014), Coté et al. (2019), Simonetti et al. (2019)); iii) possible gas flows, namely either gas accretion and/or gas outflow. In both in- and out-flows the chemical enrichment is less than in absence of them, since the accreted gas is generally metal poor and therefore it dilutes the metals already present in the interstellar medium (ISM), and the outflows subtract gas from the system, thus lowering the SFR and therefore the chemical enrichment. Equations containing all these sources must be written for each studied chemical element. Abundance ratios are

particularly important tools, since different elements are produced by different stars with different lifetimes. Therefore the ratio of one element produced fastly, such as oxygen, and one produced on a large range of timescales, such as iron, can be used as a cosmic clock. The interpretation of such ratios as functions of the stellar metallicity, $[\text{Fe}/\text{H}]$, is known as *time-delay model* (Matteucci (2012)), and allows us to reconstruct the history of star formation, as we will see in the next Sections.

2. The time delay-model

In Figure 1 we show an illustration of the so-called time-delay model (see Matteucci (2012)). In particular, we show the $[\alpha/\text{Fe}]$ versus $[\text{Fe}/\text{H}]$ relation, as predicted by the time-delay model for the solar vicinity. We see that the $[\alpha/\text{Fe}]$ ratio is almost constant during the early Galactic phases ($[\text{Fe}/\text{H}] \leq -1.0$ dex), due to the almost sole contribution of core-collapse SNe (CC-SNe) to chemical enrichment, while for $[\text{Fe}/\text{H}] > -1.0$ dex the ratio starts decreasing due to the appearance of the Type Ia SNe which produce the bulk of Fe. In Figure 2, are instead plotted the predictions of the $[\alpha/\text{Fe}]$ versus $[\text{Fe}/\text{H}]$ relations in objects suffering different histories of star formation: the upper curve refers to the predictions for the galactic bulge, the median curve to the solar neighbourhood and the lower one to an irregular galaxy, such as the LMC. While the knee in the solar vicinity occurs at $[\text{Fe}/\text{H}] \sim -1.0$ dex, in the case of the Galactic bulge, where the SFR is assumed to be much more efficient, it occurs at a larger value of $[\text{Fe}/\text{H}]$. This is due to the fact that a very efficient SFR means a large amount of CC-SNe which do produce part of the Fe, although much less than SNeIa, which is enough to increase the gas metallicity very fast and move the knee value to higher metallicities. The contrary occurs for irregular galaxies, which are supposed to have a much milder SFR than the solar vicinity: in this case, the knee is moved at lower $[\text{Fe}/\text{H}]$ than in the solar neighbourhood. This diagram is a very useful tool to understand the morphological type of high-redshift not resolved galaxies for which we know only the chemical abundances.

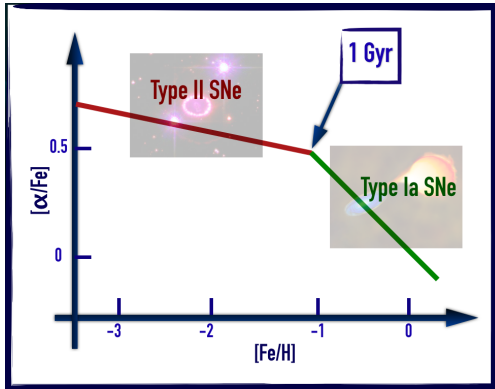


Fig. 1. A sketch of the $[\alpha/\text{Fe}]$ vs. $[\text{Fe}/\text{H}]$ to illustrate the time-delay model in the solar neighbourhood.

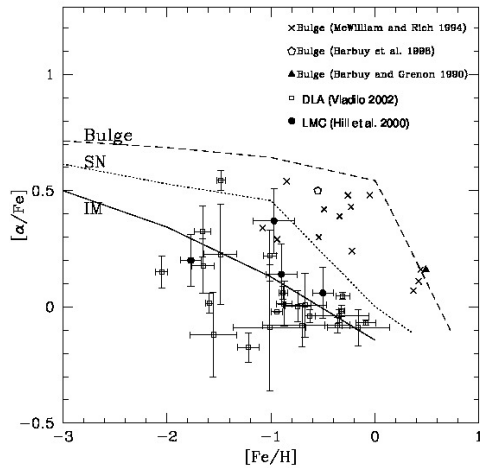


Fig. 2. The $[\alpha/\text{Fe}]$ vs. $[\text{Fe}/\text{H}]$ plot for different galaxies. The curves are the predictions of models assuming the same stellar yields but different star formation histories. The reference to the data and the Figure are from Matteucci (2012).

3. The main Galactic stellar populations

Our Galaxy, the Milky Way, has four main stellar populations: halo, bulge, thick and thin-disk ones. The halo population is made of metal poor stars ($[\text{Fe}/\text{H}] \leq -1.0$ dex) generally showing oversolar $[\alpha/\text{Fe}]$ ratios. The origin of halo stars is still controversial, since some of the stars might have formed *in situ*

and some might have been accreted from interactions with satellite galaxies (e.g. Mackereth & Bovy (2020), Iorio & Belokurov (2021)). The thick disk stellar population has a metal content in the range $-1.0 < [\text{Fe}/\text{H}] \leq -0.6$ dex, while the stellar population of the thin disk has $[\text{Fe}/\text{H}] > -0.6$ dex, which can reach even $[\text{Fe}/\text{H}] \sim +1.0$ dex. Finally, the bulge stars have metallicity in the range $-2.0 \leq [\text{Fe}/\text{H}] \leq +1.0$ dex. The kinematics of halo and bulge stars is similar and reflects that of spheroids, whereas the kinematics of the stars in the thin disk shows circular and regular orbits. The thick disk stars have instead a kinematics in between that of the halo and thin disk stars. The most recent spectroscopic Galactic Surveys, such as APOGEE (Majewski et al. (2017)), AMBRE (de Laverny et al. (2012)), Gaia-ESO (Gilmore et al. (2012), Gilmore et al. (2022)) and APOKASC (APOGEE + Kepler Asteroseismology Science Consortium, Silva Aguirre et al. (2018)), distinguish the thick and thin-disk stars by means of their chemical pattern, thus attributing to the thick disk the α -enhanced stars. From these data, a dichotomy in the $[\alpha/\text{Fe}]$ abundance patterns of thick and thin disk stars is evident. In the AMBRE and Gaia-ESO (GES) surveys, for example, the $[\alpha/\text{Fe}]$ ratios in the two disks lie in two almost parallel sequences, whereas in APOGEE and APOKASC data the above mentioned ratios in the thin disk seem to lie in a flatter sequence. Some models have been suggested to explain this double sequence of $[\alpha/\text{Fe}]$ ratios, as well will show in the next Section.

4. Possible models to explain the observed $[\alpha/\text{Fe}]$ bimodality in the thick and thin disk

Recent data have shown a clear bimodality in the relation $[\alpha/\text{Fe}]$ vs. $[\text{Fe}/\text{H}]$ for the thick and thin disk stars (see Figures 3 and 4).

Possible models for explaining such a bimodality can be summarized as follows:

– The two-infall model

The thick disk forms first with a sort a starburst triggered by accretion of extragalactic

tic gas, then followed by the formation of the thin disk due to a second infall episode occurring more slowly and with less efficient star formation. In between the formation of the two disks the SFR is extremely low and almost negligible for a period lasting roughly 1 Gyr. In Figure 3 upper panel it is indicated the gap in the star formation. This scheme was originally suggested by Chiappini et al. (1997) who applied it to the halo-thick disk and thin disk.

– The parallel model

The parallel model was suggested by Grisoni et al. (2017) and consists in assuming that the thick and thin disk form by means of two independent episodes of gas accretion, occurring almost in parallel and not sequentially as in the two-infall scheme.

– Stellar migration

It has been suggested the possibility that the thick disk was formed by stars migrated from the inner regions (e.g. Anders et al. (2017), Buck (2020)).

In Figure 3, we present the predictions of the two-infall and parallel model compared to AMBRE data, which show that the thick disk stars (red dots) are α -enhanced and extend up to $[\text{Fe}/\text{H}] \leq -0.5$ dex, while the thin disk stars (grey dots) show lower $[\alpha/\text{Fe}]$ ratios and extend up to $[\text{Fe}/\text{H}] \sim +1.0$ dex. There are also some stars (blue dots), whose origin is not clear: they could be either metal rich thick disk stars, as predicted by the parallel model (lower panel), or they could be stars migrated from the inner regions, which is the only possible explanation if one adopts the two-infall model (upper panel).

In Figure 4, we show the comparison of a revised two-infall model by Spitoni et al. (2019), where the gap between the formation of the thick and thin disk is ~ 4 Gyr. The model is compared to APOKASC data. In this case, the $[\alpha/\text{Fe}]$ ratios of thin disk stars decrease between $[\text{Fe}/\text{H}] = -0.4$ and -0.2 dex and then run almost flat as functions of $[\text{Fe}/\text{H}]$. This behaviour is well explained by the occurrence of the the second primordial gas infall episode, which dilutes by the same amount

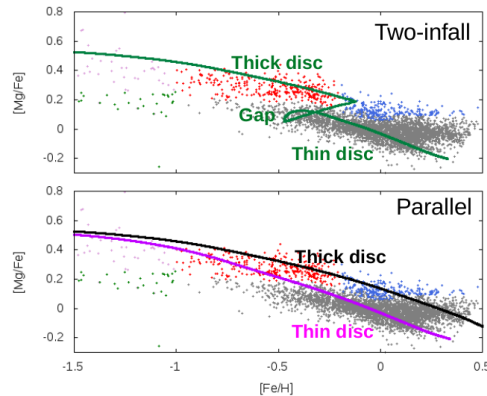


Fig. 3. $[\text{Mg}/\text{Fe}]$ vs. $[\text{Fe}/\text{H}]$ relations for thick and thin disk: a comparison between the predictions of the parallel and two-infall models with AMBRE data. See description in the text. From Grisoni et al. (2017).

both α -elements and Fe. Then when star formation starts in the thin disk, the α -elements increase thus increasing the $[\alpha/\text{Fe}]$ ratio which then declines again when SNe Ia start polluting the ISM with Fe (see also Spitoni & Matteucci, this conference, for a more extensive discussion). This behaviour of the ratios result in the loop seen in Figure 4. The long quenching in the star formation suggested by the Spitoni et al. (2019) model could be explained as due to the major merger episode with Gaia-Enceladus which occurred several Gyrs ago, as suggested by Vincenzo et al. (2019). On the other hand, the parallel model does not reproduce, as well as the two-infall model, the APOKASC data, while it is acceptable for GES and AMBRE data (see Grisoni et al. (2017)), as we have previously shown.

5. The formation and evolution of the bulge

Galactic archaeology suggests that the bulge, a spheroid of $\sim 10^{10} M_{\odot}$ with a radius of ~ 2 Kpc at the center of the Milky Way, evolved very quickly and its stars formed during a fast and intense burst of star formation. Two main stellar populations have been identified in the bulge: one with enhanced $[\alpha/\text{Fe}]$ ratios and metallicities up to solar, and another

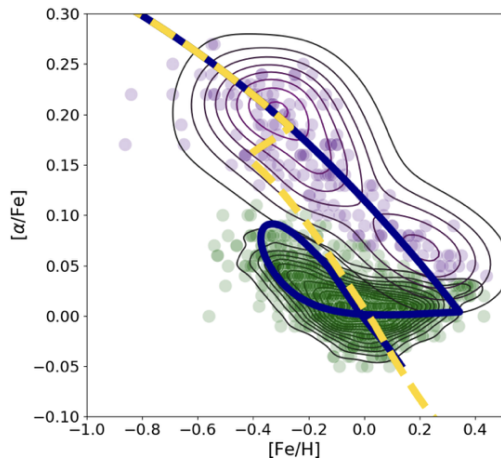


Fig. 4. Comparison between APOKASC data (Silva Aguirre et al. (2018)) for thick (magenta dots) and thin (green dots) disk stars with the model of Spitoni et al. (2019) (blue continuous line) and with the original two-infall model of Chiappini et al. (1997) (yellow dashed line). The loop seen in the blue line is due to the effect of the second infall episode, as described in the text. Note that in the classical two-infall model the gap in star formation was much shorter (1Gy), thus producing a much smaller loop.

with higher metallicities and lower $[\alpha/\text{Fe}]$ ratios. The origin of these two populations is still under debate and it could be explained in two ways: i) the metal rich population formed after a first intense burst of star formation followed by a gap in the SFR of roughly 250 Myr, or ii) the metal rich population is made of stars accreted from the innermost regions of the disk (Matteucci et al. (2019)). In Figure 5 we show the GES data (Rojas et al. (2017)) relative to the metallicity distribution function (MDF) of the bulge stars. In this Figure it is evident the presence of two stellar populations, as described before. Overimposed to the data are models with a gap in the SFR of different length (from 50 to 500 Myr), and the best one is that with a gap of 250 Myr. The models all assume a very intense SFR, almost 20 times more efficient and an initial mass function (IMF) more top-heavy than in the solar vicinity. In Figure 6, the predicted $[\text{Mg}/\text{Fe}]$ vs. $[\text{Fe}/\text{H}]$ relation for the bulge is presented to-

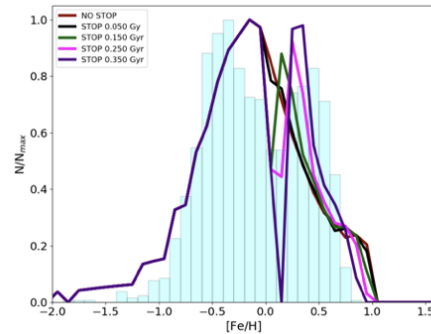


Fig. 5. Metallicity distribution function for bulge stars from GES data (Rojas et al. (2017)). Overimposed to the data are model predictions where a gap in the star formation of different length has been assumed. Figure and models from Matteucci et al. (2019).

gether with GES data. As one can see, the gap in the SFR is not immediately evident in the $[\text{Mg}/\text{Fe}]$ ratios, but a density plot of the same data (lower panel) shows that a gap might indeed exist.

6. The evolution of Lithium in the Milky Way

As a final example of Galactic archaeology I would like to discuss the evolution of ${}^7\text{Li}$ in the Galaxy, as well as what is called the “cosmological lithium problem”. This element is formed in part during the Big Bang and in part by stars during galaxy evolution. In particular, the main identified Li producers are AGB and RG stars, novae, cosmic rays and perhaps CC-SNe. In D’Antona & Matteucci (1991) it was suggested that novae could be important Li producers, especially to reproduce the behavior of the abundance of Li vs. $[\text{Fe}/\text{H}]$ in the Milky Way. In this kind of diagram (Rebolo et al. (1988)) the data show an initial plateau, where the Li abundance is practically constant (the well known Spite plateau), which extends between $[\text{Fe}/\text{H}] \sim -3.0$ and ~ -1.0 dex. For stars of lower metallicity the situation is not so clear. For $[\text{Fe}/\text{H}] > -1.0$ dex, the Li abundance increases up to the value observed in meteorites.

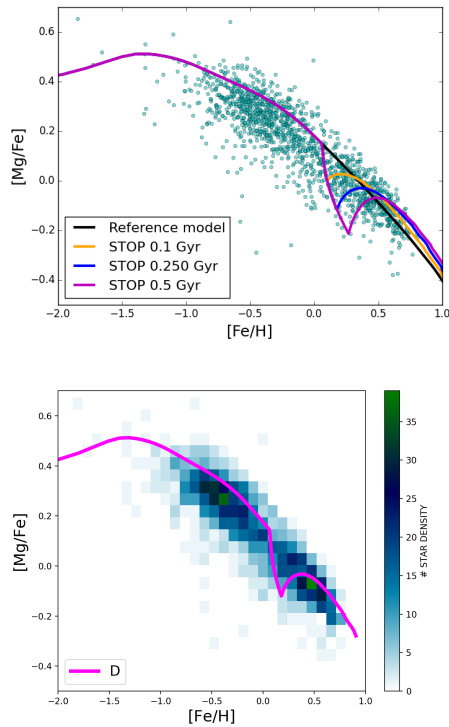


Fig. 6. The bulge $[Mg/Fe]$ vs. $[Fe/H]$ relation: comparison between GES data and models of chemical evolution of the bulge. In the upper panel are shown model predictions with different SFR gaps, while in the lower panel is shown a density plot of the best model (250 Myr gap) and the data. The models are from Matteucci et al. (2019).

A peculiar feature of this diagram is that the evolution of Li is traced by the upper envelope of the data, which shows the original Li abundance in stars and therefore that of the ISM at the time of their birth, whereas all the stars below the upper envelope do not show the original Li abundance. In fact, Li is easily depleted in stars for temperatures $> 2.8 \cdot 10^6$ K. All of this can be seen in Figure 7, where we show the data for Li and models of galactic chemical evolution as a comparison. The steep rise of Li abundance for $[Fe/H] > -1.0$ dex can be at best reproduced if one assumes novae as Li producers, although the Li nucleosynthesis calculations in novae still suffer of many un-

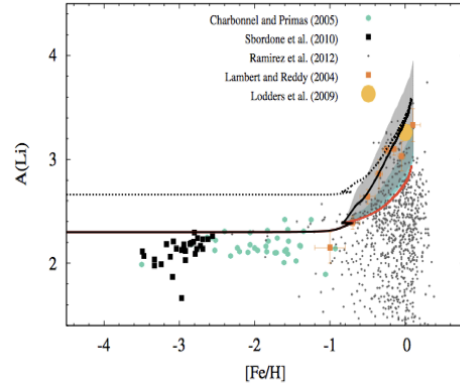


Fig. 7. The Li abundance versus $[Fe/H]$: a comparison between data and models. The model predictions are represented by the lines. The upper black dotted line assumes a primordial Li value as suggested by Planck, whereas the continuous lower line refers to a primordial Li abundance equal to the value of the Spite plateau and includes novae as main Li producers. The orange continuous line refers to a model without the nova contribution (only AGB stars and cosmic rays).

certainties. Few years ago, Izzo et al. (2015) claimed the first detection of Li lines in novae, thus reinforcing that prediction. In Cescutti & Molaro (2019) it was suggested that novae can be the sole producers of ${}^7\text{Li}$. However, there is another problem concerning Figure 7, and in particular the fact that before the results of WMAP and PLANCK the Li abundance in the Spite plateau was the same as the predicted primordial Li abundance ($12+\log(\text{Li}/\text{H}) \sim 2.2$ dex), whereas with the last results from the study of the Cosmic Microwave Background the primordial Li is a factor of 3 higher (see Coc et al. (2014)), as shown in Figure 7. A possible explanation is that the Li has been depleted by the same amount in metal poor stars, irrespective of their metallicity and effective temperature. Even more puzzling is that also in dwarf satellites of the Milky Way there is a precise Spite plateau at the same level as in halo stars (see Matteucci (2021b) for a discussion), that suggests that perhaps a revision of the standard ΛCDM model could be also necessary in the future.

7. Conclusions

In summary, thanks to the cosmic clocks represented by abundance ratios of elements produced on different timescales, such as α -elements and Fe, we can infer the timescales for the formation of the different Galactic stellar components: halo, bulge, thick and thin disk. Galactic archaeology suggests that the inner halo formed quickly while the outer halo probably formed by accretion of stars from satellite galaxies. The bulge formed very quickly the bulk of its stars (on roughly 1 Gyr, Matteucci et al. (2019)), and also the thick disk formed on a timescale no longer than 2 Gyr (Grisoni et al. (2017); Spitoni et al. (2019)), whereas the thin disk formed on a much longer timescale of several Gyrs (Chiappini et al. (1997); Grisoni et al. (2017); Spitoni et al. (2019)). A rather long gap in the SFR between the end of the thick disk phase and the beginning of the thin disk formation can explain the bimodality in the APOKASC data relative to $[\alpha/\text{Fe}]$ ratios in the thick and thin disk.

Stellar migration from the innermost disk regions can have contributed to the observed bimodality in $[\alpha/\text{Fe}]$ ratios as suggested by several authors (Anders et al. (2017); Buck (2020); Palla et al. (2022)).

More high resolution spectroscopic data for different chemical elements are necessary to better constrain both the stellar nucleosynthesis and mechanism of formation of the various stellar Galactic component.

I would like to conclude by thanking again Margherita Hack for her pioneering works on stellar spectroscopy and for setting a wonderful example for women in science.

Acknowledgements. I am grateful to all my collaborators, V. Grisoni, M. Palla, D. Romano, S. Spitoni, whose work made possible this review.

References

- Anders, X., Chiappini, C., Minchev, I., et al. 2017, *A&A*, 600, 70
- Buck, T. 2020, *MNRAS*, 491, 5435
- Cescutti, G., Molaro, P. 2019, *MNRAS*, 482, 4372
- Chiappini, C., Matteucci, F., Gratton, R. 1997, *ApJ*, 477, 765
- Coc, A., Uzan, J.P., vangioni, E. 2014, *JCAP*, 10, 50
- Coté, B., Eichler, M., Arcones, A., et al. 2019, *ApJ*, 875, 106
- D'Antona, F., Matteucci, F. 1991, *A&A*, 248, 62
- de Laverny, P., Recio-Blanco, A., et al. 2012, *A&A*, 544, 126
- Gilmore, G., Randich, S., Asplund, M. 2012, *The Messenger*, 147, 25
- Gilmore, G., Randich, S., Worley, C.C., et al. 2022, *A&A*, 666, 120
- Grisoni, V., Spitoni, E., Matteucci, F., et al. 2017, *MNRAS*, 472, 3637
- Iorio, G., Belokurov, V. 2021, *MNRAS*, 502, 5686
- Izzo, L., Della Valle, M., Mason, E., et al. 2015, *ApJ*, 808, L14
- Mackereth, J.T., Bovy, J. 2020, *MNRAS*, 492, 3631
- Majewski, S.R., Schiavon, R.P., et al. 2017, *AJ*, 154, 94
- Matteucci, F. 2012, *Chemical Evolution of Galaxies: Astronomy and Astrophysics Library*. ISBN 978-3-642-22490-4. Springer-Verlag Berlin Heidelberg, 2012
- Matteucci, F., Romano, D., et al. 2014, *MNRAS*, 438, 2177
- Matteucci, F. 2021a, *A&ARv*, 29, 5
- Matteucci, F., Molaro, M., Aguado, D., Romano, D. 2021b, *MNRAS*, 505, 200
- Matteucci, F., Grisoni, V., Spitoni, E., et al. 2019, *MNRAS*, 487, 5363
- Palla, M., Santos-Peral, P., Recio-Blanco, A., et al. 2022, *A&A*, 663, 125
- Rebolo, R., Molaro, P., Beckman, J.E. 1988, *A&A*, 192, 192
- Rojas-Arriagada, A., Recio-Blanco, A., de Laverny, P., et al. 2017, *A&A*, 601, 140
- Silva Aguirre, V., Bojsen-Hansen, M., et al. 2018, *MNRAS*, 475, 5487
- Simonetti, P., Matteucci, F., Greggio, L., Cescutti, G. 2019, *MNRAS*, 486, 2896
- Spitoni, E., Silva Aguirre, V., Matteucci, F., et al. 2019, *A&A*, 623, 60
- Vincenzo, F., Spitoni, E., Calura, F., et al. 2019, *MNRAS*, 487, L47